

INFLUENCE OF ACTIVATED BIOMASS FLY ASH ON PORTLAND CEMENT HYDRATION

#RIMVYDAS KAMINSKAS, VYTAUTAS CESNAUSKAS

*Department of Silicate Technology, Faculty of Chemical Technology,
Kaunas University of Technology, Kaunas, Lithuania*

#E-mail: rimvydas.kaminskas@ktu.lt

Submitted June 20, 2014; accepted November 23, 2014

Keywords: Portland cement, Pozzolana, Microfiller, Biomass fly ash, Hydration

This study investigated the possibility of using biomass fly ash as an additive for ordinary Portland cement (OPC), where 5 %, 10 %, 15 %, and 25 % (by weight) of the Portland cement was replaced with biomass fly ash (BFA) and tribochemically activated biomass fly ash (AFA). The mixture was then hardened for 28 days in water at 20°C. It is estimated that both additives are distinguished for very low pozzolanic activity. Under normal conditions, the BFA additive had a negative effect on the strength properties of cement. After 28 days of hydration, the compressive strength of samples with 15 wt. % BFA additive was more than 10 % lower than that of OPC (54 MPa), whereas the compressive strength of the sample with 25 wt. % additive (35 MPa) was 30 % lower than that of the OPC. Additional milling of biomass fly ash samples changes the particle size distribution and composition of the compounds. Tribochemically activated biomass fly ash additive significantly accelerates the hydration process of calcium silicates and had a positive effect on the strength properties of the samples, because up to 15 wt. % of the cement can be replaced with this additive without impairing the strength properties of Portland cement. Also, activated biomass fly ash impedes the alkali-silica reaction in cement mortars.

INTRODUCTION

In recent years, pressures on the global environment and energy security have led to an increasing demand for renewable energy sources and diversification of Europe's energy supply. Among these resources, biomass could play an important role because it is considered a renewable and CO₂-neutral energy resource once the consumption rate is lower than the growth rate and can potentially provide energy for heat, power, and transports from the same installation [1].

The characteristics of ashes from biomass combustion vary widely and depend on the cleanliness of the biomass fuel, combustion technology, the collection location, and other factors [2, 3]. Therefore, the biomass composition can be highly variable depending on the geographic locations and industrial processes. The chemical composition of biomass fly ash is an important property to consider as a supplementary cementing material in blended cement. The general term "the activity of additives" defines the chemical activity (usually pozzolanic activity) and microfiller effect. The pozzolanic activity is the ability to react with portlandite (Ca(OH)₂) in the presence of an excess of water, which is expressed in the quantity of bound CaO mg per 1 g of additive. Moreover, the microfiller effect depends mainly on the shape and size of the particles, the particle size distribution, and specific surface area [4].

Many kinds of biomass fly ash have pozzolanic properties similar to coal fly ash, such as those from rice husk, wood, wheat straw, and sugar cane straw [5-7], some of which have been added in concrete as mineral admixtures, improving the performance of concrete. Further study of pozzolanic reaction kinetics has found that at one month of curing, coal fly ash (Class C and F) and biomass fly ash (either cofired or wood fly ash by itself) have undergone significant pozzolanic reactions at ambient temperatures [8]. On the other hand, some data published in the literature [9] shows that the chemical composition of wood ash indicates very high LOI, high alkali content, and very low SiO₂ values (and hence do not satisfy the requirements to be classified as Class N pozzolans). The authors also state that a high SiO₂ content in the biomass ash does not automatically imply an effective pozzolanic material (high efficiency factor).

It is known that a higher quantity of water is used for waste wood ash concrete [10, 11]. The compressive strength increases with duration, but it decreases with the use of more additive. It was determined that the compressive strength of waste wood ash concrete is lower than that of concrete without additives [12-14]. This can be explained by the different behavior of waste wood ash, because it acts more as a microfiller in concrete matrix than as a binder. Tkaczewska et al. [15] found that, during hydration, the cement samples, which contain coal and biomass fly ash, show lower heat

flow values, a higher quantity of $\text{Ca}(\text{OH})_2$, and slower C_3S hydration in comparison with samples containing bituminous coal fly ash as an additive.

The aim of this work is to investigate the influence of biomass fly ash (wood chips and waste wood) on the hydration and hardening processes of Portland cement.

EXPERIMENTAL

The fly ashes used in the experiment were from a biomass (wood chips and waste wood)-fired power plant in Lithuania. The main chemical composition and characteristics of the biomass fly ash are shown in Table 1. Ordinary Portland cement CEM I 42.5 R was used in this work. The chemical composition of the cement is shown in Table 1. The mineralogical composition of the clinker was as follows: $3\text{CaO}\cdot\text{SiO}_2$ 57.80 wt. %; $2\text{CaO}\cdot\text{SiO}_2$ 22.15 wt. %; $3\text{CaO}\cdot\text{Al}_2\text{O}_3$ 6.65 wt. %; and $4\text{CaO}\cdot\text{Al}_2\text{O}_3\cdot\text{Fe}_2\text{O}_3$ 13.40 wt. %.

Table 1. Chemical composition and characteristics of raw materials.

Component (wt. %)	Biomass fly ash	Portland cement
SiO_2	45.08	20.8
Al_2O_3	2.98	5.7
Fe_2O_3	1.37	4.4
CaO	16.58	61.9
MgO	1.90	1.0
K_2O	4.47	–
Na_2O	0.37	0.9
MnO	0.56	–
SO_3	2.26	2.5
P_2O_5	2.07	–
TiO_2	0.2	–
ZnO	0.12	–
BaO	0.10	–
Loss on ignition	8.89	0.4
Specific surface area ($\text{m}^2\cdot\text{kg}^{-1}$)	310	350

Samples were formed of pure ordinary Portland cement and Portland cement with 5 %, 10 %, 15 %, and 25 % (by weight) replacement with fly ash. The consistency of the cement paste and the initial and final setting times of the cement were estimated according to European Standard EN 196-3. Samples for compressive strength analysis (prisms $4 \times 4 \times 16$ cm) were formed according to European Standard EN 196-1 (the cement-to-sand ratio was 1:3, and the water-to-cement ratio was 0.5). During the first day, the samples were kept in moulds at $20 \pm 1^\circ\text{C}$ and 100 % humidity. After 24 hours of formation, the samples were transferred to deionized water and stored there for 27 days at $20 \pm 1^\circ\text{C}$. In order to make a more exact estimation of the hydration process,

the samples for instrumental analysis were prepared without the sand that is usually used. The storage conditions of the samples were analogous to those used during the strength test. The hydration of the samples was stopped using acetone.

The pozzolanic activity was assessed using the modified Chapelle method. This test consists of placing 1.000 g of a mineral admixture into 500 ml of a lime solution ($1.200 \text{ g}\cdot\text{l}^{-1} \text{ CaO}$). The solutions were kept for the first 48 h in a thermostat at 45°C . At the end of this period, 50 ml of the solution was taken, and the CaO content was determined by titration with 0.05 N hydrochloric acid (HCl) solution using methyl orange as the indicator. The results were expressed in milligrams of fixed CaO per gram of pozzolanic additive. The rest of the solution (450 ml) was again kept for 24 h at 45°C . The process was repeated until the estimated value of the pozzolanic activity was insignificantly low (7 days).

For the alkali-silica reaction test, reactive quartzitic fine gravel is used as the aggregate. The aggregate is ground down to 0.125 mm, and the comminuted material is used to produce a mortar ($4 \times 4 \times 16$ cm mortar prisms). The binder-to-aggregate ratio was 1:3, and the water-to-binder ratio was 0.5. Samples were formed of pure ordinary Portland cement and Portland cement with 5 %, 15 %, and 25 % (by weight) replacement with biomass fly ash. During the first day, the samples were kept in moulds at $20 \pm 1^\circ\text{C}$ and 100 % humidity. After removal from the moulds, the bars were transferred to storage containers filled with 1 N NaOH solution maintained at $80 \pm 1^\circ\text{C}$. The lengths of the mortar bars were periodically measured over a 14-day period. The expansion value was calculated as the average percentage length change of three mortar bar samples based on length change since initial immersion in NaOH.

The XRD analysis was performed using the D8 Advance diffractometer (Bruker AXS, Karlsruhe, Germany) operating at the tube voltage of 40 kV and tube current of 40 mA. The X-ray beam was filtered with a Ni 0.02 mm filter to select the $\text{CuK}\alpha$ wavelength. Diffraction patterns were recorded in a Bragg-Brentano geometry using a fast counting detector Bruker LynxEye based on silicon strip technology. The specimens of samples were scanned over the range $2\theta = 3 - 70^\circ$ at a scanning speed of $6^\circ\cdot\text{min}^{-1}$ using a coupled two theta/theta scan type.

Simultaneous thermal analysis (STA) (differential scanning calorimetry and thermogravimetry) was carried out on a Netzsch STA 409 PC Luxx instrument with ceramic sample handlers and crucibles of Pt-Rh. At a heating rate of $15^\circ\text{C}\cdot\text{min}^{-1}$, the temperature ranged from 30°C to 1000°C under the ambient atmosphere.

Infrared spectra were measured using a Perkin-Elmer Fourier transform infrared (FT-IR) system Spectrum X spectrometer. Samples were prepared by mixing 1 mg of the sample in 200 mg of KBr. The spectral analysis was performed in the range of $4000 - 400 \text{ cm}^{-1}$ with a spectral resolution of 1 cm^{-1} .

The particle size distribution of fly ash was measured by a CILAS 1090 LD laser scattering particle size distribution analyzer. An amount of 0.1 g of powdered sample was put in 100 ml of ethanol and underwent dispersion treatment by an ultrasonic dispersion unit for 70 s.

The chemical composition analysis of samples were performed by X-ray fluorescence spectroscopy (XRF) on a Bruker X-ray S8 Tiger WD spectrometer equipped with a Rh tube with energy of up to 60 keV. Powder samples were measured in a helium atmosphere, and the data were analyzed with SPECTRA Plus QUANT EXPRESS standardless software.

The calorimetric analysis data were gathered using a TAM AIR III calorimeter. The range of measurement was ± 600 mW, the sensitivity of the signal was $4 \mu\text{W}$, the time constant was < 500 s, the temperature of the experiment was $25 \pm 0.1^\circ\text{C}$, and the water-to-solid ratio was 0.5.

RESULTS AND DISCUSSION

In order to monitor the trend of variation of the elements in the biomass fly ashes, a number of samples were collected over several months and were analysed for chemical composition using the XRF technique. The results are shown in Figure 1. A variation of the absolute maximum of around 20 % is observed in the distribution of major elements. The variations can be attributed to the variation in the operating conditions as well as the biomass fuels used for the combustion.

For further research, the sample for which the chemical composition is given in Table 1 was chosen (Sample 1). The loss on ignition was 8.89 wt. %. The organic content as well as the decomposition of calcite is the reason for the loss on ignition.

The particle size distribution of biomass fly ash (BFA) measured by laser diffraction is shown in Figure 2. The Blaine value of the BFA powder is $310 \text{ m}^2 \cdot \text{kg}^{-1}$. The

particle size of BFA estimated by laser diffraction is inaccurate because a significant portion of the particles are larger than $500 \mu\text{m}$.

The results of the sieve analysis are shown in Table 2. The data of Figure 2 and Table 2 show that BFA particle diameter varies over very wide limits, and particles larger than $80 \mu\text{m}$ constitute 78.34 wt. % of the total amount.

Table 2. Sieve analysis results of biomass fly ash.

Sieve size (μm)	Mass residue (g)	Percent residue	Cumulative percent
600	0.33	11	11
425	0.23	7.69	18.69
212	0.97	32.33	51.02
106	0.65	21.66	72.68
80	0.17	5.66	78.34
< 80	0.65	21.66	100
BFA Mass (g)	3.00	100	–

In the next stage of the research the pozzolanic activity investigation was carried out. It was established that the pozzolanic activity of BFA was very low and reached only 22 mg CaO/g. The data confirm that the biomass fly ash properties can be highly variable depending on geographic location and industrial processes because many authors [16-19] note high biomass fly ash pozzolanic activity.

Investigation of the compressive strength of the samples, in which the content of BFA additive varied from 5 to 25 wt. %, showed that this additive had a negative effect on the strength properties of cement. It was estimated (Figure 3) that after 7 days of hydration, all samples with BFA additive had lower compressive strength than OPC samples. When hydration time was increased to 28 days, the compressive strength of the samples with BFA additive remained lower than that of the OPC samples. It should be noted that the compressive

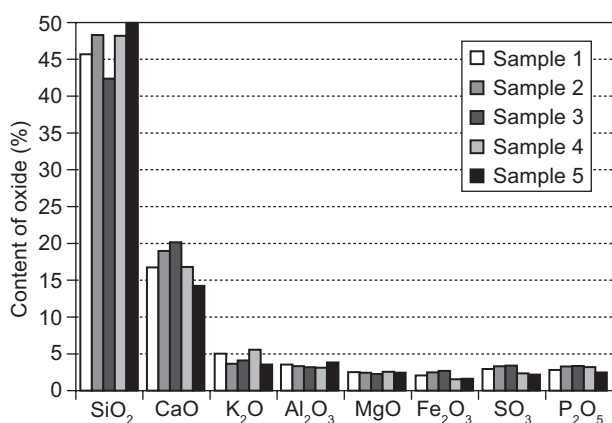


Figure 1. Variation of chemical composition of the biomass fly ash samples.

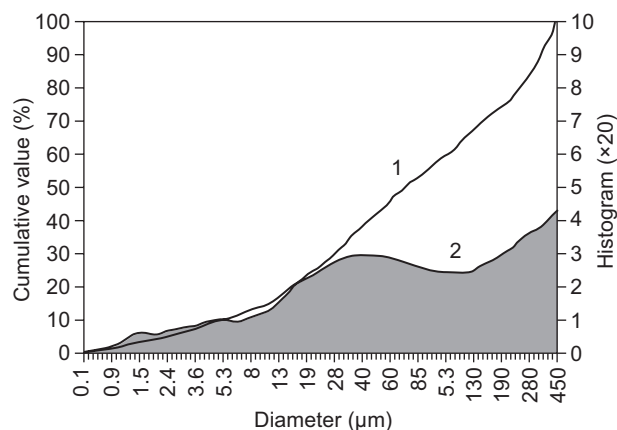


Figure 2. Particle size distribution of biomass fly ash (BFA).

strength of samples with 15 wt. % BFA additive was more than 10 % lower than that of OPC (53 MPa), whereas the compressive strength of the sample with 25 wt. % additive after 28 days of hydration (35 MPa) was 30 % lower than that of the OPC. Thus, the investigated biomass fly ash (as-received) is an unsuitable additive for Portland cement because it has a negative influence on the strength properties of the OPC.

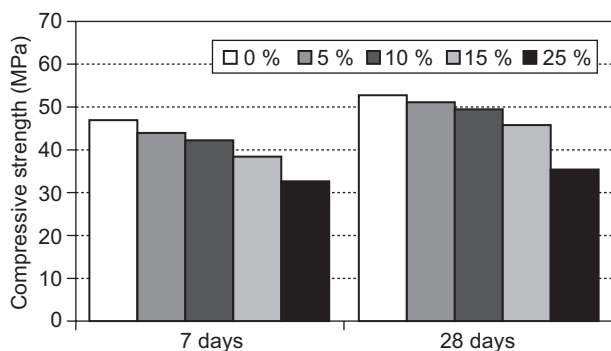


Figure 3. Compressive strength of cement samples with different amounts of BFA additive after 7 and 28 days of hydration.

According to the obtained experimental results, it was decided in the next stage of research to grind BFA, which can then be used as microfiller. The BFA was ground using a vibrating disc mill to a specific surface area of $430 \text{ m}^2\text{kg}^{-1}$.

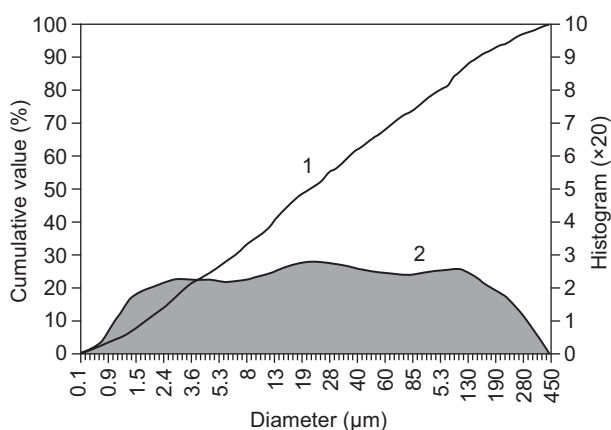


Figure 4. Particle size distribution of additionally milled biomass fly ash (AFA).

The particle size distribution of additionally milled biomass fly ash (AFA) is shown in Figure 4. After milling, 100 wt. % of the particles are lower than $450 \mu\text{m}$, and the uniformly distributed particles are dominated by diameters less than $63 \mu\text{m}$, constituting 70 wt. % of the total amount. Thus, these prepared biomass fly ashes can be used as a microfiller (EN 12620:2003+A1:2008). It was determined that the pozzolanic activity of additionally milled biomass fly ash was higher than BFA, but it remained very low and reached only 30 mg CaO/g .

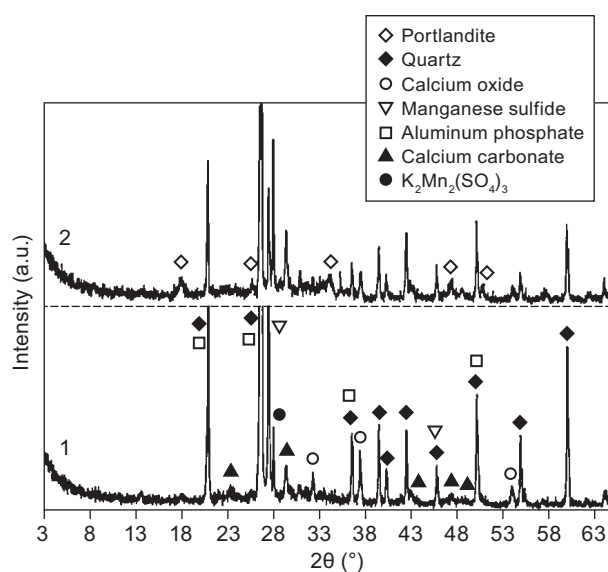


Figure 5. X-ray diffraction pattern of biomass fly ash; 1 – fly ash as-received (BFA), 2 – ground fly ash (AFA).

According to the XRD analysis data (Figure 5, curve 1), quartz (d -spacing: 0.425 ; 0.334 ; 0.181 nm ; JCPDS 77-1060), CaO (d -spacing: 0.277 ; 0.240 ; 0.169 nm ; JCPDS 82-1690), MnS (d -spacing: 0.324 ; 0.198 nm ; JCPDS 40-1288), Al_3PO_4 (d -spacing: 0.423 ; 0.334 nm ; JCPDS 76-228), and calcite (d -spacing: 0.302 ; 0.228 ; 0.209 ; 0.189 ; 0.186 nm ; JCPDS 72-1650) were found in BFA. After milling of BFA samples, the intensity of the quartz and Al_3PO_4 peaks considerably decrease, and new peaks characteristic of portlandite (d -spacing: 0.489 ; 0.262 ; 0.192 nm ; JCPDS 44-1481) were found in AFA samples (Figure 5, curve 2). Portlandite formation can be explained by the fact that during the grinding process CaO becomes very active, joins the environmental humidity, and becomes portlandite. Thus, grinding of BFA results not only in mechanical fly ash particle milling, but it also changes the composition of the compounds; therefore this process can be called a tribochemical activation of biomass fly ash.

The results of the XRD data were confirmed by STA and FT-IR data (Figures 6 and 7). In the DSC curve of the AFA sample, three significant endothermic effects at 440°C , 575°C , and 705°C were found, which are attributed to the decomposition of portlandite, α -modification quartz converting to β -modification, and decomposition of calcite, respectively.

In the FT-IR curve of the AFA sample the absorption maximum characteristic of portlandite at 3644 cm^{-1} frequency was observed [20]. The absorption bands of calcium carbonate that are described by the stretching $\nu_3\text{-CO}_3^{2-}$ (713 cm^{-1}), $\nu_2\text{-CO}_3^{2-}$ (875 cm^{-1}), and $\nu_3\text{-CO}_3^{2-}$ (1430 cm^{-1}) vibrations were also visible in the spectrum [21]. The infrared spectra of silicate in the range $1200 - 400 \text{ cm}^{-1}$ are classified into four characteristic bands around 1000 (overlapped), 780 , 695 , and 450 cm^{-1} in the standard quartz spectra. Among these four

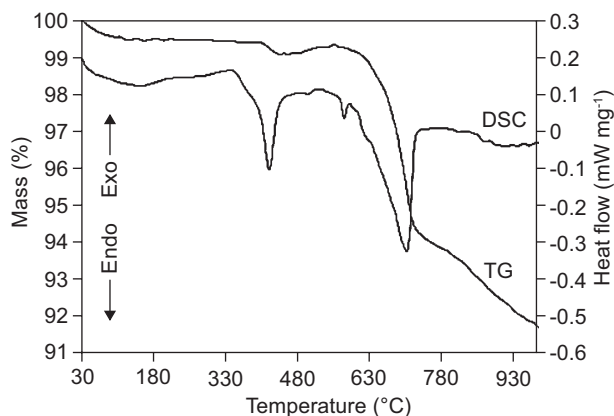


Figure 6. STA curves of activated fly ash (AFA) sample.

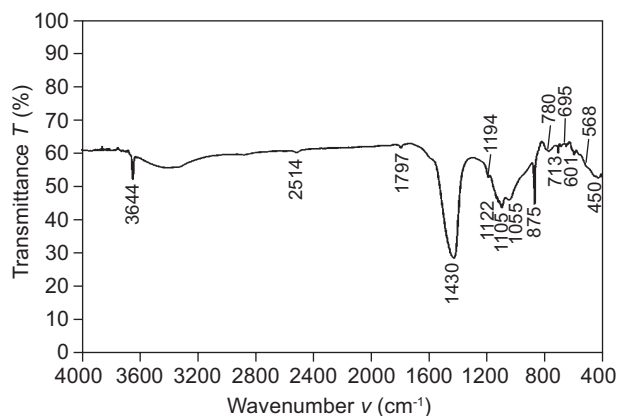


Figure 7. FT-IR curve of AFA sample.

characteristic peak regions, the peak at 695 cm^{-1} is unique to the crystalline materials [22]. The band observed in the FT-IR spectrum around 1122 cm^{-1} corresponding to the symmetric stretching mode of $[\text{PO}_4]^{3-}$ is specific for Al_3PO_4 [23]; the presence of two characteristic bands around 568 and 601 cm^{-1} correspond to the ν_4 (O–P–O) bending mode [24]. The frequencies ν_1 , ν_2 , ν_3 , and ν_4 of the SO_4^{2-} ion occur at 983 (overlapped), 450 , 1105 , and 611 cm^{-1} , respectively [25]. An absorption band characteristic of MnS can't be identified, because metal-sulphide stretching vibrations occur below 400 cm^{-1} [26].

In the next stage of research the influence of AFA additive on the cement hydration process was investigated. The results of physical tests—setting time and normal consistency of different cement compositions—are summarised in Table 3. Taking these data into account, a negligible increase of the setting time and a continuous increase of the normal consistency according to the increasing percentage of added AFA additive were determined. This is explained by the partial substitution of cement by adding a character with fly ash, causing excessive consumption of water and absorption of part of the water for hydration.

Investigation of the compressive strength of the samples, in which the content of AFA additive varied from 5 to 25 wt. %, showed that this additive had a positive effect on the strength properties of cement. It was estimated (Figure 8) that after 7 days of hydration, samples with 5 and 10 wt. % AFA additive had higher strength, whereas samples with 15 wt. % AFA additive had the same compressive strength (46.8 MPa) as OPC

samples. When hydration time was increased to 28 days, the compressive strength of the samples with 5–15 wt. % AFA additive is higher than that of the OPC samples. It should be noted that even for samples with 25 wt. % AFA additive the compressive strength was less than 10 % lower (48.3 MPa) than that of the OPC samples (53 MPa). Thus, the tribochemically activated biomass fly ash is an available additive for Portland cement because up to 15 wt. % of the cement can be replaced with this additive without impairing the strength properties of Portland cement.

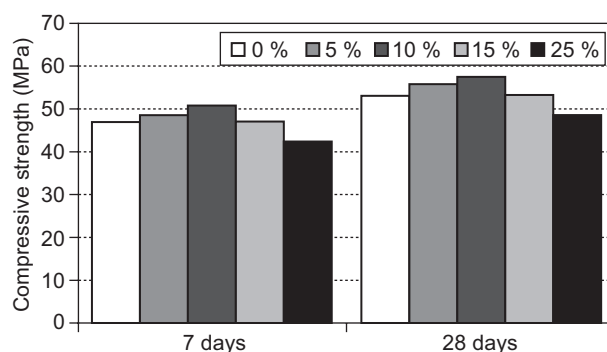


Figure 8. Compressive strength of cement samples with different amounts of AFA additive after 7 and 28 days of hydration.

Table 3. Influence of AFA on normal consistency and setting time of portland cement.

Amount of additive (wt. %)	Normal consistency (W/C*) (%)	Setting time (min)	
		initial	final
0	0.255	89	139
5	0.265	95	153
15	0.275	105	155
25	0.285	104	160

In order to assess the influence of fly ash additive on the initial hydration of cement, a measurement of heat evolution during the hydration process (calorimetric analysis) was performed (Figure 9). As shown in Figure 9, two sharp peaks of heat evolution on the calorimetric curve of cement were noted: the first indicates the active evolution of heat due to wetting a powder of cement and the initial kinetic reaction, during which Ca^{2+} , OH^- , SiO_4^{4-} , and SO_4^{2-} ions pass into the solution, and the second has to do with the reaction between the deeper layers of C_3S particles and water [27, 28]. During hydration of the cement samples with AFA (except sample with 5 wt. % additive), on the released heat flow measurement curve (Figure 9a, curves 3, 4), an earlier flow of heat evolution

was identified at the second period of hydration than in the pure cement sample (Figure 9a, 1 curve). The maximum heat flow value of the sample with 15 wt. % of AFA additive was reached 5 h 50 min after the beginning of hydration. For the sample with 25 wt. % of AFA additive it was reached 5 h 30 min after the beginning of hydration, whereas for pure cement and the sample with 5 wt. % of AFA additive (Figure 9a, curves 3, 4) it was reached after 6 h 20 min. Therefore, it can be assumed that the AFA additive significantly accelerates the initial cement hydration. It is possible that during the induction period Ca^{2+} ions adsorbed on the surface of the fly ash or finely ground fly ash can act as crystallization

centers, around which portlandite and calcium silicate hydrate begin to crystallize. In both cases, the Ca^{2+} concentration reduces in the solution, and due to this the cement hydration accelerates [27, 28]. All of the samples with AFA additive up to 70 h of hydration emit less heat energy (Figure 9b, curves 2-4). This can be explained by the fact that the AFA additive doesn't have binding or pozzolanic properties; therefore the hydration with less cement emits less heat energy.

The results of XRD analysis showed (Figure 10a) that after 7 days of hydration, in all X-ray patterns of samples, the diffraction peaks of unhydrated tricalcium silicate (d -spacing: 0.304; 0.277; 0.260; 0.218 nm; JCPDS 42-551)

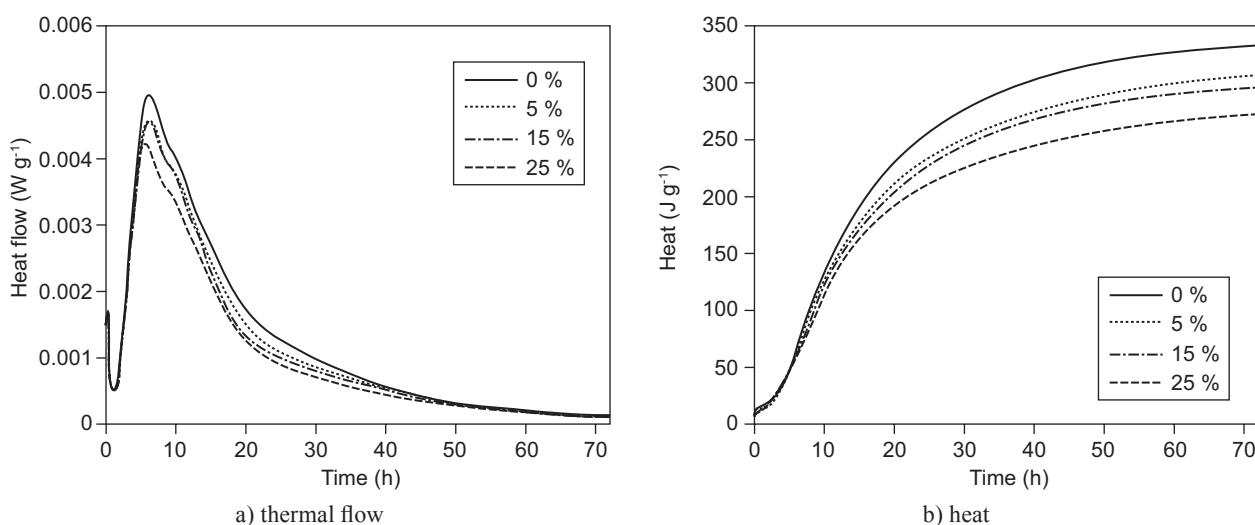


Figure 9. Calorimetric curves of thermal flow a) and heat b) in samples with different amounts of AFA additive.

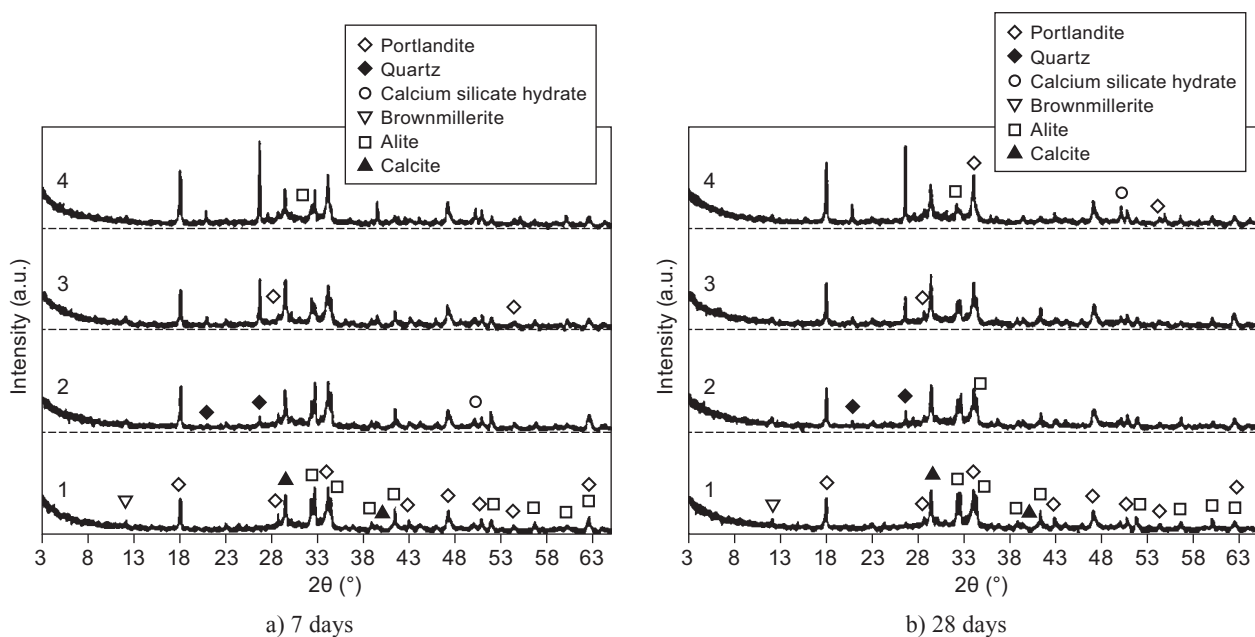


Figure 10. X-ray diffraction patterns of cement samples with AFA additive cured for 7 a) and 28 b) days under normal conditions: 1 – pure Portland cement; 2 – Portland cement with 5 wt. % additive; 3 – Portland cement with 15 wt. % additive; 4 – Portland cement with 25 wt. % additive.

and unhydrated brownmillerite (*d*-spacing: 0.725 nm; JCPDS 30-226) were identified. Also, the ordinary product of cement hydration, portlandite (*d*-spacing: 0.489; 0.262 nm; JCPDS 44-1481), was identified in all curves. It was determined that, after 7 days of hydration, peaks of silica dioxide (*d*-spacing: 0.425; 0.334 nm; JCPDS 77-1060) were visible only in samples with fly ash (Figure 10 a, curves 2-4), because quartz is an integral part of this additive. In addition to the main products in XRD curves, the characteristic peaks of CaCO₃ (*d*-spacing: 0.302; 0.189; 0.186 nm) were observed. The peak of calcium carbonate in the samples is related to the carbonization process of them, and a negligible content of CaCO₃ is an integral part of cement (up to 5 wt. %) and biomass fly ash. It should be noted that a low-intensity characteristic peak of calcium silicate hydrate (*d*-spacing: 0.305; 0.271; 0.190 nm; JCPDS 3-588) was identified in the XRD curves of the samples with AFA additive (Figure 10 a curves 2-4).

After 28 days of hydration the nature of the XRD curves remains similar to the curves after 7 days of hydration: peaks characteristic of portlandite, unhydrated C₃S, CSH, CaCO₃, and quartz were identified in the curves. The intensity of unhydrated tricalcium silicate diffraction peaks was slightly reduced in the cement sample (Figure 10b, curve 1). Meanwhile, in the samples

with 5 and 15 wt. % of AFA additive the reduction was greater, and in the samples with 25 wt. % of AFA additive, only a trace of unhydrated C₃S was observed. It should be noted that the intensity of peaks characteristic of CSH and portlandite grows with an increasing amount of AFA additive in the samples. The higher intensity of the diffraction peaks of portlandite may be associated with a more intense hydration process of calcium silicate and with portlandite as one of the AFA components; however, the higher intensity of CSH peaks can be attributed only to the more intense hydration process of calcium silicates.

In all DSC curves of hydrated samples (Figure 11), three significant endothermic peaks in the temperature ranges of 100 – 200°C, 440 – 460°C, and 725 – 760°C were observed. The endothermic peak at 100 – 200°C is due to the dehydration of most cement hydration products (calcium silicate hydrates, calcium aluminates, ettringite, etc.), whereas those at 440 – 460°C and 725 – 760°C indicate the decomposition of portlandite and calcium carbonate, respectively.

The results of TG analysis (Table 4) showed that when the amount of AFA additive was increased, after 7 days of hydration the mass loss due to the presence of portlandite (~ 455°C) was also increased. The higher mass loss was also prominent on the samples with AFA

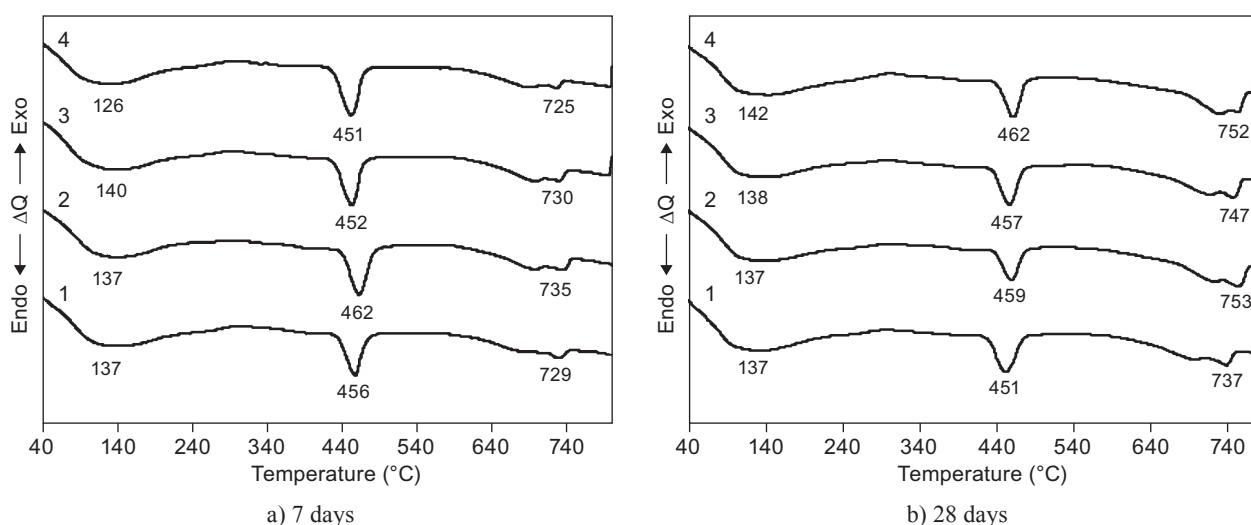


Figure 11. Differential scanning calorimetry patterns of cement samples with AFA additive cured for 7 a) and 28 b) days under normal conditions: 1 – pure Portland cement; 2 – Portland cement with 5 wt. % additive; 3 – Portland cement with 15 wt. % additive; 4 – Portland cement with 25 wt. % additive.

Table 4. Thermogravimetry analysis results of samples cured for 7 and 28 days under normal conditions.

Amount of AFA additive (wt. %)	Mass loss (wt. %)					
	After 7 days of hydration			After 28 days of hydration		
	100 – 140°C	~ 455°C	680 – 760°C	100 – 140°C	~ 455°C	680 – 760°C
0	1.58	1.83	3.66	1.68	2.0	4.69
5	1.61	1.85	4.09	1.72	2.16	5.05
15	1.70	1.91	4.61	1.81	2.24	5.12
25	1.74	2.15	4.65	2.08	2.67	5.25

additive in the area of calcium silicate hydrate dehydration (90 – 140°C). A clear tendency was observed: when the amount of AFA additive increases in the samples, the mass loss in decomposition areas of portlandite and calcium silicate hydrates also increases. This confirmed the assumption that AFA additive promoted the hydration of calcium silicates. It should be noted that this tendency remains for the samples cured for 28 days under normal conditions. Even in the sample with 25 wt. % of additive a larger amount of portlandite and CSH were formed than in the OPC sample. Considering that 25 % less calcium silicates were hydrated in this sample (cement was replaced by AFA), the TG analysis results showed a significant acceleration of the calcium silicate hydration process. This influence of AFA additive explained a

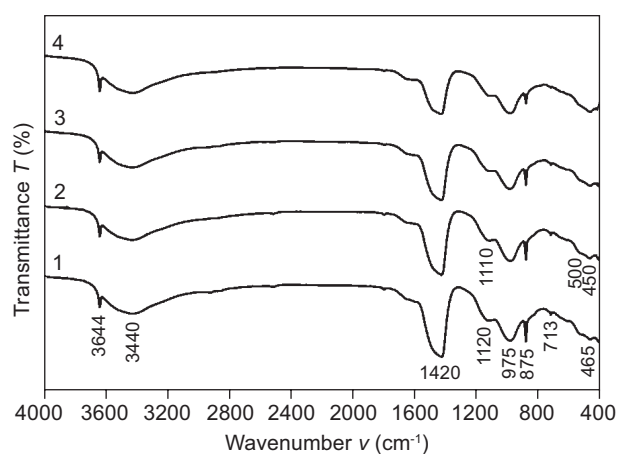
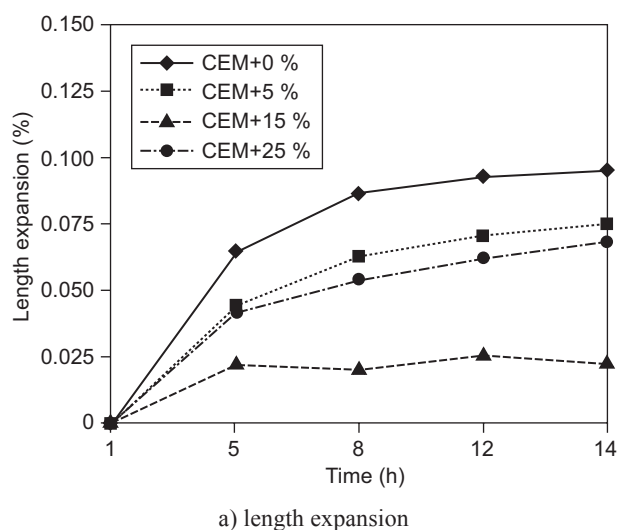


Figure 12. FT-IR curves of cement samples with AFA additive cured for 28 days under normal conditions: 1 – pure Portland cement; 2 – Portland cement with 5 wt. % additive; 3 – Portland cement with 15 wt. % additive; 4 – Portland cement with 25 wt. % additive.



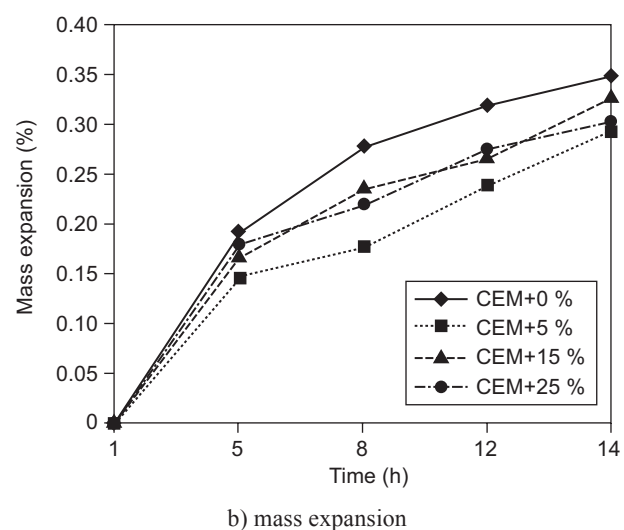
a) length expansion

higher compressive strength of the samples with additive (up to 15 wt. %) after 7 and 28 days of hydration. It should be noted that in samples with AFA additive greater amounts of both hydration products (CSH and portlandite) were formed, which indicates that in these samples a pozzolanic reaction doesn't occur—otherwise part of the CH would react with active SiO_2 and the amount of CH should decrease.

After 28 days of hydration, in the FT-IR curves (Figure 12) of all samples the absorption band characteristic of portlandite at 3644 cm^{-1} frequency was observed. The wide absorption band at $\sim 3440 \text{ cm}^{-1}$ frequency is assigned to valence $\nu(\text{H}_2\text{O})$ vibrations. The absorption band at 975 cm^{-1} frequency is characteristic of $\nu(\text{Si-O})$ vibrations, which identifies calcium silicate hydrates, whereas $\sim 465 \text{ cm}^{-1}$ is characteristic of the internal $\delta[\text{SiO}_4]^{4-}$ tetrahedral deformations. The absorption bands characteristic of calcium carbonate at 713 cm^{-1} , 875 cm^{-1} , and 1420 cm^{-1} also were observed in FT-IR curves of all samples.

In FT-IR curves of the samples with AFA additive the intensity of the absorption band of portlandite (3644 cm^{-1}) was higher than in the pure cement sample. Also, the intensity of absorption bands at 973 cm^{-1} and especially at 465 cm^{-1} in the samples with AFA additive was higher than in the pure cement sample. This confirms the previous statement that portlandite and calcium silicate hydrate were formed more completely in the samples with AFA additive.

The absorption band shoulder at $\sim 1120 \text{ cm}^{-1}$, characteristic of $\delta(\text{S-O})$ vibrations in $[\text{SO}_4]^{2-}$ groups and assigned to ettringite [29], was observed in the pure cement sample. Meanwhile, in the samples with AFA additive, the intensity of absorption bands characteristic of S-O vibrations in sulfates were reduced and displaced to a lower wavelength range ($\sim 1110 \text{ cm}^{-1}$) typi-



b) mass expansion

Figure 13. Length expansion a) and mass expansion b) of cement samples with AFA additive after 14 days of storage in 1 molar NaOH solution at 80°C .

cal of monosulfoaluminate [30]. This shows that AFA additive promotes recrystallization of ettringite to monosulfoaluminate. It is possible that the SO_4^{2-} ions, like Ca^{2+} ions, were adsorbed on the surface of ground biomass fly ash particles.

Because biomass fly ash contains a number of alkalis, in the next stage of research the influence of AFA additive on the course of the alkali-silica reaction in cement mortars was determined. It was found that the mass of all investigated samples during maintenance in 1 M NaOH solution at 80°C for up to 14 days (Figure 13b) increased exponentially; however, in samples with an AFA additive the mass gain was less than in the pure OPC sample. The reduced mass increase is probably due to the fact that the addition of AFA additive provides a better grain-size composition in the mixture and a denser cement stone structure. The biggest change in length (Figure 13a) is also observed in the pure cement sample (0.095 %), while in samples with AFA additive the length expansion is less and varies from 0.088 % (sample with 25 wt. % additive) to 0.023 % (sample with 15 wt. % additive). It was observed that the expansion rate of all mortars was high in the initial stages, and after that it seemed to decrease. According to the applied methodology, the critical value of length expansion is 0.1 %. Thus, the expansion of the reference mortar prepared with the OPC was only slightly less than the critical value; meanwhile, the expansion results for mortar mixtures containing activated biomass fly ash showed a reduction in the expansion compared to the plain cement mortars.

CONCLUSIONS

1. The investigated biomass fly ash (as-received) is distinguished by an uneven grain-size composition and very low pozzolanic activity and had a negative effect on the strength properties of Portland cement samples. After 28 days of hydration, the compressive strength of samples with 15 wt. % BFA additive was more than 10 % lower than that of OPC (54 MPa), whereas compressive strength of the sample with 25 wt. % additive (35 MPa) was 30 % lower than that of the OPC.
2. After additional milling of biomass fly ash samples, the particles were distributed uniformly, particle diameters less than 63 μm constituted 70 wt. % of the total amount, and it changes the composition of the compounds.
3. Tribochemically activated biomass fly ash additive significantly accelerates the hydration process of calcium silicates and has a positive effect on the strength properties of samples, because up to 15 wt. % of the cement can be replaced with this additive without impairing the strength properties of Portland cement.

4. Activated biomass fly ash impedes the alkali-silica reaction in cement mortars.

REFERENCES

1. Rajamma R., Ball R.J., Tarelho L.A.C., Allen G.C., Labrincha J.A., Ferreira V.M.: *J. Hazard. Mater.* **172**, 1049 (2009).
2. Yin C., Rosendahl L.A., Kaer S.K.: *Prog. Energy Combust. Sci.* **34**, 725 (2008).
3. Obernberger I., Biedermann F., Widmann W., Riedl R.: *Biomass Bioenergy* **12**, 211 (1997).
4. Shvarzman A., Kovler K., Schamban I., Grader G.S., Shter G.E.: *Adv. Cem. Res.* **13**, 1 (2001).
5. Martirena F., Middendorf B., Day R.L., Gehrke M., Roque P., Martínez L., Betancourt S.: *Cem. Concr. Res.* **36**, 1056 (2006).
6. Yu Q., Sawayama K., Sugita S., Shoya M., Isojima Y.: *Cem Concr. Res.* **29**, 37 (1999).
7. Naik T.R., Kraus R.N.: *Concr. Int.* **25**, 55 (2003).
8. Wang S., Dalton R., Bragonje S., Tullis J., Baxter L. in: *Kinetics of pozzolanic reaction and strength build-up in the mortar of biomass/coal fly ash with calcium hydroxide*, p. 99-110, Ed. Malhotra V. M., American Concrete Institute, Miami 2007.
9. Demis S., Rodrigues C.S., Santos L.A., Papadakis V.G. in: *Proc. XIII DBMC - 13th International Conference on Durability of Building Materials and Components*, Sao Paulo, Brazil; 2013 (available online: www.researchgate.net/publication/260287514_An_investigation_of_the_effectiveness_and_durability_characteristic_of_biomass_ashes_as_pozzolanic_materials).
10. Udoeyo F.F., Inyang H., Young D.T., Oparadu E.E.: *J. Mater. Civ. Eng.* **18**, 605 (2006).
11. Fehrs J.E. in: *Ash from the combustion of treated wood: characterization and management options*. The National Bioash Utilization Conference, Portland, 1996.
12. Etiegni L. in: *Wood ash recycling and land disposal*, p. 174, Thesis Ph.D., Department of Forest Products. University of Idaho at Moscow, Idaho, 1990.
13. Abdullahi M.: *Leonardo El. J. Pract. Technol.* **89**, (2006).
14. Wang S., Miller A., Llamazos E., Fonseca F, Baxter L.: *Fuel*, **87**, 365 (2008).
15. Tkaczewska E., Malolepszy J.: *Constr. Build. Mater.* **23**, 2694 (2009).
16. Wang S., Baxter L.: *Fuel Process. Technol.* **88**, 1165 (2007).
17. Elinwa A.U., Mahmood Y.A.: *Cem. Concr. Compos.* **24**, 219 (2002).
18. Cheah C.B., Ramli M.: *Resour. Conserv. Recycl.* **55**, 669 (2011).
19. Naik T.R.: *Tests of wood ash as a potential source for construction materials* (Report No. CBU-1999-09), p. 1-61, UWM Center for By-Products Utilization, Department of Civil Engineering and Mechanics, University of Wisconsin-Milwaukee, Milwaukee, 1999.
20. Ylmen R., Jaglid U., Steenari B.M., Panas I.: *Cem. Concr. Res.* **39**, 433 (2009).
21. Stepkowska E.T.: *J. Therm. Anal. Calorim.* **84**, 175 (2006).
22. Saikia B.J., Parthasarathy G., Sarmah N.C.: *Bull. Mater. Sci.* **31**, 775 (2008).
23. Hepzi Pramila Devamani R., Alagar M.: *Int. J. Appl. Sci. Eng. Res.* **1**, 769 (2012).
24. Paz A., Guadarrama D., López M., Gonzalez J.E., Brizuela N., Aragón J.: *Quim. Nova.* **35**, (2012).
25. Bensted J.: *Naturwiss.* **63**, 193 (1976).
26. Dhanam M., Kavitha B., Shanmugapriya M.: *Chalcogenide Letters.* **6**, 541 (2009).
27. Langan B.W., Weng K., Ward M.A.: *Cem. Concr. Res.* **32**, 1045 (2002).
28. Snelson D.G., Wild S., O'Farrell M.: *Cem. Concr. Res.* **38**, 832 (2008).
29. Fernández-Carrasco L., Torrens-Martín D., Morales L.M., Martínez-Ramírez S.: *Infrared Spectroscopy in the Analysis of Building and Construction Materials*, p. 369-382, InTech, Croatia 2012.
30. Taylor H.F.W.: *Cement Chemistry*, 2nd edition, p. 361, Thomas Telford Publishing, London 1997.